Wireless Real-Time Monitoring of Ablation using a Wearable Antenna

Ahmet Bilir, Mehmet Emre Korkmaz, Sema Dumanli*
*Bogazici University, Electrical and Electronics Engineering, Istanbul, Turkey, sema.dumanli@bogazici.edu.tr

***Abstract*—Accurate monitoring of the ablated area size is crucial in microwave ablation therapy to prevent insufficient or excessive tissue ablation. In this paper, we utilize the changes in the electrical properties of tissues during ablation to achieve real-time monitoring. The proposed system comprises a microwave applicator, designed as a coaxial slot antenna, and an on-body antenna. As the ablation progresses, the rising temperature alters the electrical properties of the tissues surrounding the applicator, which in turn affects the transmission coefficient between the applicator and the on-body antenna. The effectiveness of this method is validated through recursive thermal and electromagnetic simulations in a hepatic tumor scenario. The results demonstrate that while the reflection coefficient of the applicator converges after a certain point, the phase of the transmission coefficient continues to change, offering a promising method for tracking the size of the ablated area.**

***Index Terms*—microwave ablation, recursive thermal and EM simulation, real-time monitoring, wearable antenna.**

I. Introduction

Microwave ablation (MWA) therapy is a minimally invasive technique used to treat malignant tissues. Although surgical procedures like resection are the standard approach for treatment, ablation systems are often preferred when surgery is not feasible [1]. In MWA, high-power electromagnetic waves are used to heat the target tissue, raising its temperature to a level that destroys the malignant cells.

The basic principle of MWA involves inserting a needle-like antenna into the target tissue, guided by imaging techniques such as computed tomography (CT) to precisely locate the tumor. Once positioned, high power is delivered to the antenna, which emits electromagnetic waves into the tissue. The changing polarization of the electric field within these waves forces polar molecules, such as water, within the tissue to align with the field. This continuous realignment causes the tissue to heat up due to molecular vibration [2]. When the tissue reaches the ablation temperature, typically around 60°C, the malignant cells are effectively destroyed.

MWA is capable of producing large ablation zones in a short period of time, making real-time monitoring of the ablated area essential [3]. Clinically, this is usually achieved through ultrasound or CT imaging. However, gas bubbles formed in the tissue during MWA can interfere with ultrasound imaging, leading to inaccuracies [1]. Similarly, real-time CT imaging, which relies on detecting dark areas in the scan, may also provide low-accuracy results [4].

To address these limitations, several alternative modalities have been proposed for imaging and tracking the ablated area. Some techniques utilize the temperature-dependent electrical properties of human tissue. During ablation, the temperature of the target tissue can rise to 60-100°C, resulting in changes to its relative permittivity and conductivity. These changes can be used to track the size of the ablated area. In [4], for instance, the microwave applicator functions as both the ablation device and the sensing antenna. As ablation progresses, the relative permittivity near the antenna tip decreases significantly due to the rising temperature. This change is tracked by the antenna, but only within its near-field, limiting the monitoring to that region.

To overcome this limitation, a transmission coefficient-based method was proposed in [5] to monitor larger ablation zones. In this approach, two applicators are used to monitor and ablate the tumor. As the ablation proceeds, changes in the tissue's electrical properties can be tracked by measuring the transmission coefficient between the two antennas. This allows monitoring beyond the antenna's near-field. In this system, the ablation process is paused periodically to switch to transmission mode and measure the coefficient. A similar transmission coefficient-based technique for tracking the size of the ablated area was proposed in [6], where its effectiveness was validated through simulations involving both tumor and healthy liver tissues by the authors.

Microwave imaging based on this principle was demonstrated in [7], where an ablation applicator and 20 receiver antennas surround breast tissue for monitoring. A different method, proposed in [8], involves using an on-body antenna to monitor the ablated area size by measuring the power received during ablation. While a sweet potato was used as a liver substitute in this study, the effects of tumor presence and differences in electrical properties between the tumor and liver tissues were not considered.

In this paper, we propose a basic real-time system to monitor the ablated area during microwave ablation therapy by utilizing the transmission coefficient between the applicator and an on-body antenna. Unlike some of the previous methods, the applicator functions solely as a transmitter, and the phase of the received signal at the on-body antenna is used to track the ablated area. The effectiveness of this approach is validated through recursive thermal and electromagnetic simulations.

The paper is structured as follows: Section II outlines the thermal simulation models and methods used. The electromagnetic simulations and results are discussed in Section III. Finally, the conclusions are presented in Section IV.

II. Thermal Simulations

To characterize the ablated area as the ablation progresses, coupled simulations were conducted in a multiphysics solver. The simulation model is shown in Fig. 1. A coaxial slot antenna is used as the microwave applicator. The design and working principle of the antenna are detailed in [6]. Briefly, the ends of the outer and inner conductors of the coaxial cable are shorted, and two slits are introduced. The radii of the inner conductor, dielectric, and outer conductor are 0.1 mm, 0.33 mm, and 0.43 mm, respectively.

To expedite the simulation, the setup is modeled in 2D, as illustrated in Fig. 1. The healthy liver tissue has a radius of 50 mm and a height of 100 mm, while the tumor has a radius of 15 mm. The applicator is positioned so that both slits are located inside the tumor.

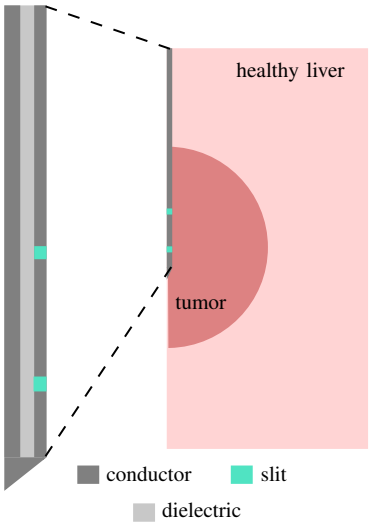

Fig. 1. The 2D simulation model used in thermal simulations.

The simulation is solved by coupling the electric field to the heating mechanism. First, the electric field inside the tissue is computed, with the input power of the applicator set at 50 W. This electric field is then fed into the bioheat module, which calculates the temperature rise based on the electric field while considering the thermal properties of the tissues and blood flow.

There are two different approaches to simulate this model. In the first approach, the initial electric field is assumed to remain constant over time, and the bioheat equation is solved using this fixed electric field. This method is referred to as 'non-recursive' throughout the paper. In the second approach, the electric field is updated at each time step. As the tissue heats and its temperature rises, the electrical properties of both the tumor and the healthy liver change, as shown in Fig. 2. Consequently, the electric field distribution within the tissues changes as well. By solving the electromagnetic equations for the updated electrical properties, this new electric field distribution is used as the input for the bioheat module at each time step. Therefore, the electric field distribution is continuously updated in response to the changing electrical properties of the tissues due to temperature changes. This approach is referred to as 'recursive' throughout the paper.

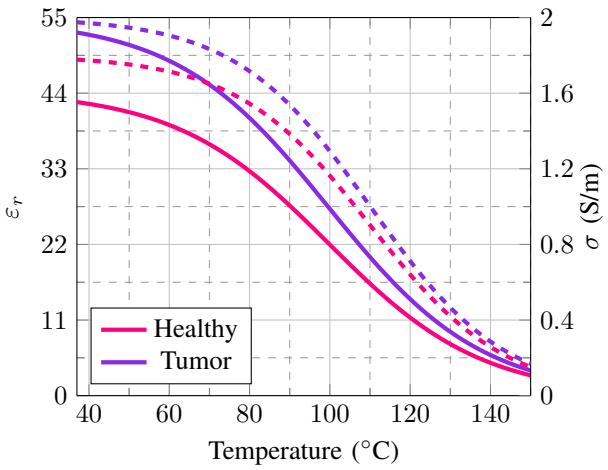

Fig. 2. The electrical properties of the healthy liver and hepatic tumor. The solid and dashed lines represent the relative permitivity and conductivity, respectively [9].

A comparison of the recursive and non-recursive simulation results when 50 W of input power is applied for 200 seconds is shown in Fig. 3. In the non-recursive simulation, the ablated area is concentrated at the applicator tip, resulting in minimal tissue damage along the applicator. In contrast, the recursive simulation shows that the ablated area is elongated along the applicator, which is due to the changing electric field at each time step, as illustrated in Fig. 4. Therefore, the non-recursive method may misrepresent the shape and size of the ablated area.

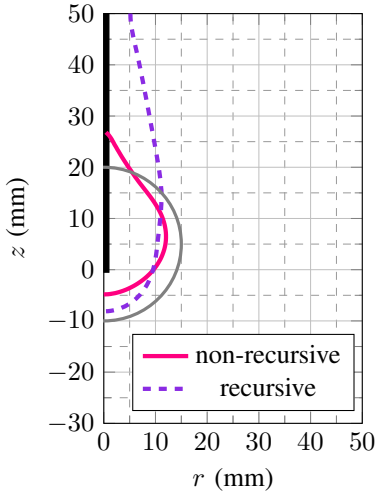

Fig. 3. The comparison between recursive and non-recursive simulations of the tissues where the temperature exceeds 60°C, after applying 50 W of input power for 200 seconds.

The size of the ablated area, defined as the tissues with a temperature exceeding 60°C, is illustrated in Fig. 5. After

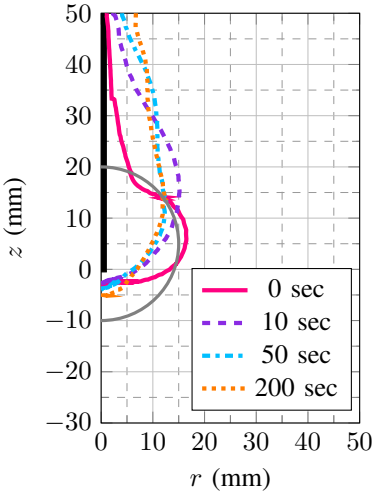

Fig. 4. The comparison of the electric field within the tissues during microwave ablation at different time points. The lines represent the electric field at 500 V/m.

approximately 200 seconds of ablation application, it is evident that the tumor has been completely ablated.

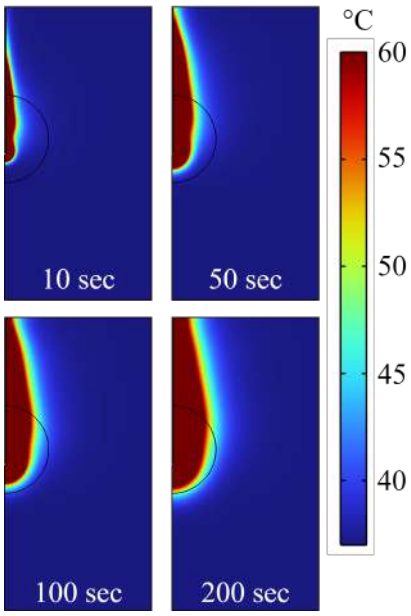

Fig. 5. The temperature maps at various time points during microwave ablation.

In Fig. 6, the change in the electrical properties of the tissues is shown. After 200 seconds of ablation, it can been that the region where the relative permittivity of the tumor is less than 30 has a radius greater than 5 mm along the applicator. Similarly, the region where the conductivity of the tissues is less than 1 S/m also exhibits a radius greater than 5 mm along the applicator after 200 seconds of ablation.

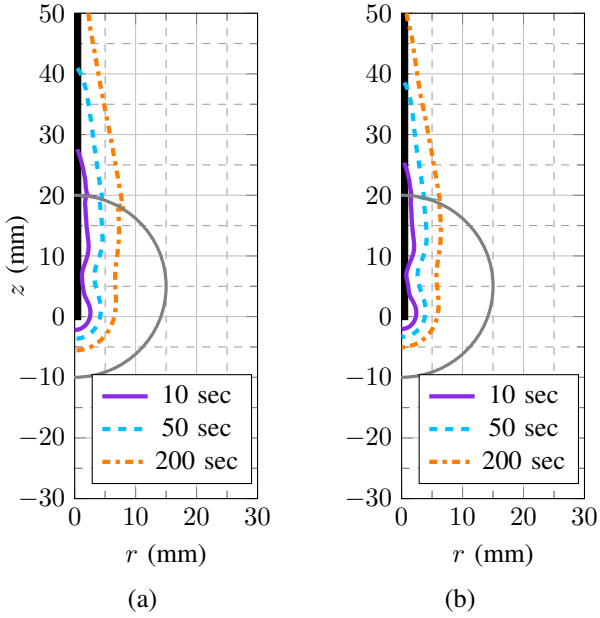

Fig. 6. The regions where (a) the relative permittivity threshold is 30, and (b) the conductivity threshold is 1 S/m during microwave ablation at various time points.

III. Electromagnetic Simulations

After conducting the recursive thermal simulations, the electrical properties of the 2D modeled tissues are exported and transformed into a 3D representation by rotating the data along the z-axis. This 3D data is then used as spatially dependent electrical properties in the electromagnetic simulations. The 3D model utilized in the electromagnetic simulations is depicted in Fig. 7. The model comprises cylindrical healthy liver tissue, a spherical tumor, the applicator, and an on-body antenna used to track the size of the ablated area. The spatially dependent electrical properties obtained from the thermal simulation are applied to both the healthy liver and tumor tissues.

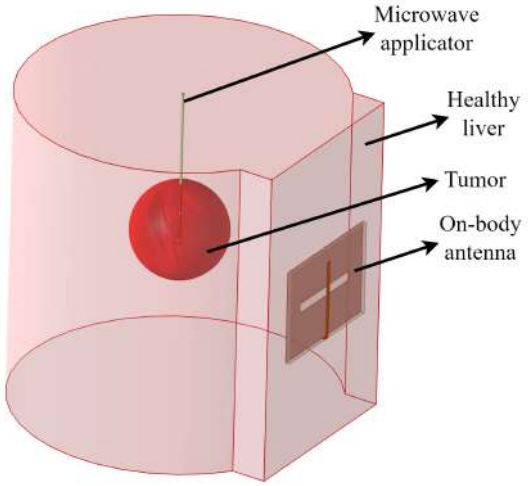

Fig. 7. The model used in the electromagnetic simulations.

A slot antenna is designed as the on-body antenna, with dimensions of 30 mm × 40 mm × 1.27 mm. The substrate selected is RO3210, a high-permittivity, low-loss dielectric, with a relative permittivity of 10.2 and a loss tangent of 0.003. To minimize near-field losses, the antenna is not placed directly in contact with the tissue; a 0.1 mm separation is introduced between the antenna and the human body. The on-body antenna is optimized to operate at 2.45 GHz. The reflection and transmission coefficients of both the applicator and the on-body antennas are shown in Fig. 8. Both antennas operate within the 2.4 GHz ISM band, and the transmission coefficient before ablation begins is approximately -45 dB at 2.45 GHz.

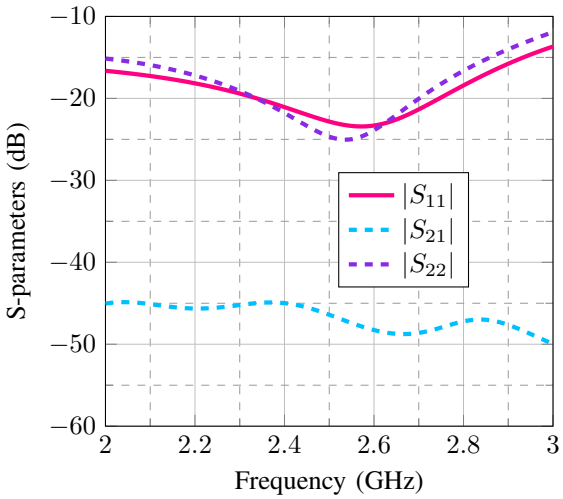

Fig. 8. The S-parameters of the antennas in Fig. 7. $|S_{11}|$ and $|S_{22}|$ are the reflection coefficients of the microwave applicator and the on-body antenna, respectively.

As the ablation progresses, the change in the reflection coefficient of the applicator is illustrated in Fig. 9. Initially, the permittivity is relatively high compared to subsequent time instances during the ablation process. As ablation continues, the permittivity of the tissues in the near field of the applicator decreases, resulting in an increase in $|S_{11}|$ of the applicator, as shown in Fig. 9 (a). At the beginning of the ablation process, $|S_{11}|$ increases drastically, but as ablation continues, it begins to converge. This convergence occurs because the electrical properties of the near field of the applicator do not change significantly after a certain time in the ablation, even though the ablated area increases. Therefore, the ablated area cannot be monitored solely by $|S_{11}|$. Similarly, the ablated area cannot be tracked by $\angle S_{11}$ for the same reason.

However, the transmission coefficient between the applicator and the on-body antenna can be used to track the size of the ablated area. The changes in the transmission coefficient as the ablation progresses are shown in Fig. 10. At the beginning of the ablation, there is a significant change in both $|S_{21}|$ and $\angle S_{21}$. As ablation continues, the magnitude of the transmission coefficient begins to converge, while the phase of the transmission coefficient continues to change.

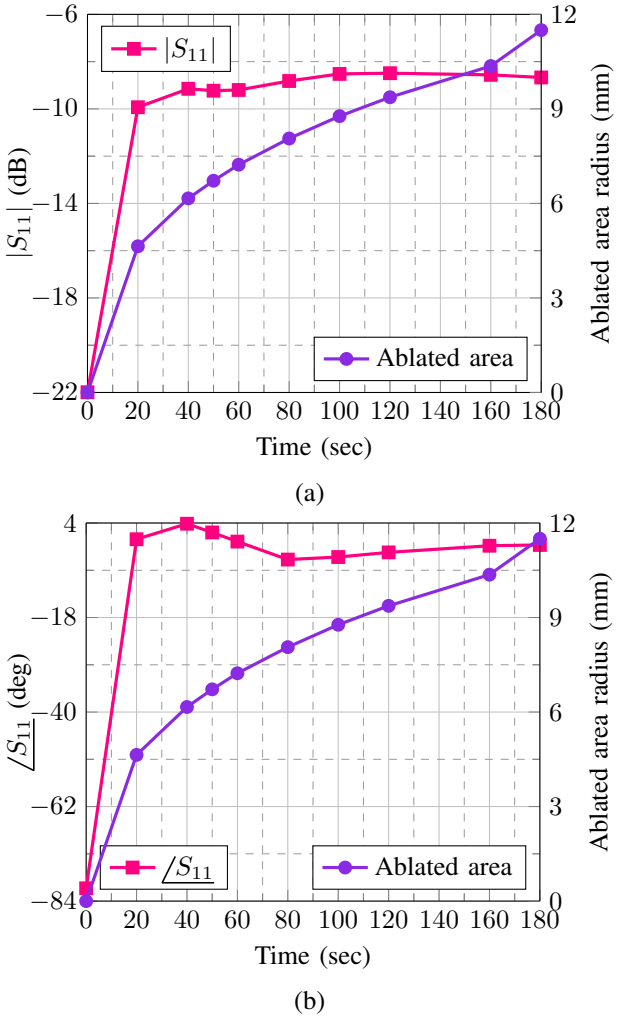

Fig. 9. The change in (a) $|S_{11}|$ and (b) $\angle S_{11}$ at 2.45 GHz as tissue ablation progresses.

Throughout the entire ablation process, the phase difference between consecutive time instances remains positive, which can be utilized to track the ablated area.

IV. Conclusion

In this paper, we proposed a real-time monitoring system for tracking the ablated area size during microwave ablation therapy. The system consists of a microwave applicator and an on-body antenna, utilizing changes in the transmission coefficient between the antennas to monitor the treatment process. The proposed method was validated through both thermal and electromagnetic simulations. In the thermal simulations, the recursive and non-recursive approaches were compared, demonstrating that non-recursive simulations may produce misleading results. The findings indicate that while the reflection coefficient of the applicator stabilizes after a certain point, the phase of the transmission coefficient continues to change, making this approach a promising method for accurately tracking the ablated area size.

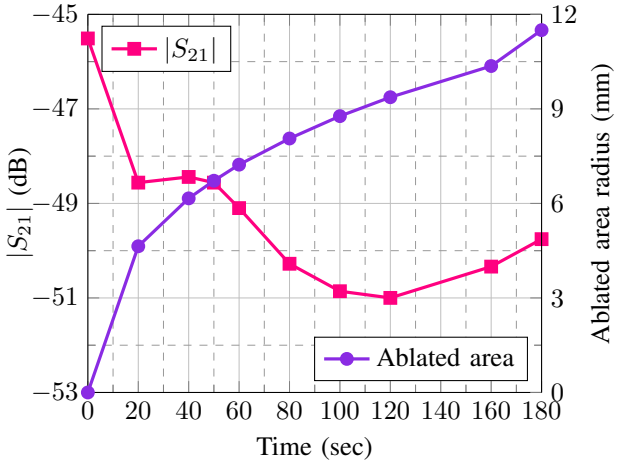

(a)

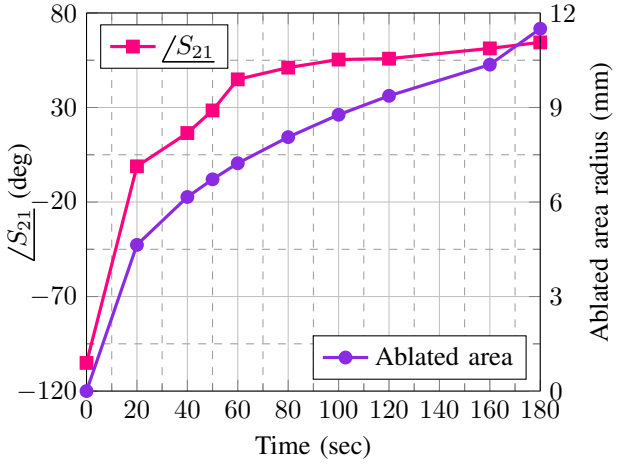

(b)

Fig. 10. The change in (a) $|S_{21}|$ and (b) $\angle S_{21}$ at 2.45 GHz as tissue ablation progresses.

REFERENCES

[1] T. Vogl, N. E. Nour-Eldin, R. Hammerstingl, B. Panahi, and N. Naguib, "Microwave ablation (MWA): Basics, technique and results in primary and metastatic liver neoplasms – review article," RöFo - Fortschritte auf dem Gebiet der Röntgenstrahlen und der bildgebenden Verfahren, vol. 189, no. 11, pp. 1055–1066, Aug. 2017. doi:10.1055/s-0043-117410.

[2] C. J. Simon, D. E. Dupuy, and W. W. Mayo-Smith, "Microwave ablation: Principles and applications," RadioGraphics, vol. 25, Oct. 2005. doi:10.1148/rg.25si055501.

[3] C. L. Brace, "Microwave Tissue Ablation: Biophysics, Technology, and Applications," Critical Reviews in Biomedical Engineering, vol. 38, no. 1, pp. 65–78, 2010, doi:10.1615/critrevbiomedeng.v38.i1.60.

[4] C. Hessinger née Reimann, B. Bazrafshan, M. Schüßler, S. Schmidt, C. Schuster, F. Hübner, T. J. Vogl, and R. Jakoby, "A Dual-Mode Coaxial Slot Applicator for Microwave Ablation Treatment," in IEEE Transactions on Microwave Theory and Techniques, vol. 67, no. 3, pp. 1255-1264, March 2019, doi: 10.1109/TMTT.2018.2880440.

[5] N. Zeinali, J. Sebek, H. Fallahi, A. Pfannenstiel and P. Prakash, "Transmission Coefficient-Based Monitoring of Microwave Ablation: Development and Experimental Evaluation in Ex Vivo Tissue," in IEEE Transactions on Biomedical Engineering, vol. 71, no. 4, pp. 1269-1280, April 2024, doi: 10.1109/TBME.2023.3331659.

[6] A. Bilir, O. K. Erden and S. Dumanli, "Coaxial Slot Antenna Array Design for Microwave Ablation and Monitoring," 2022 3rd URSI Atlantic and Asia Pacific Radio Science Meeting (AT-AP-RASC), Gran Canaria, Spain, 2022, pp. 1-4, doi: 10.23919/AT-AP-RASC54737.2022.9814337.

[7] K. Kanazawa, K. Noritake, Y. Takaishi and S. Kidera, "Microwave Imaging Algorithm Based on Waveform Reconstruction for Microwave Ablation Treatment," in IEEE Transactions on Antennas and Propagation, vol. 68, no. 7, pp. 5613-5625, July 2020, doi: 10.1109/TAP.2020.2972633.

[8] M. S. Khan, M. Hawlitzki, S. M. Taheri, G. Rose, B. Schweizer, and A. Brensing, "Investigation of Microwave Ablation Process in Sweet Potatoes as Substitute Liver," Sensors, vol. 21, no. 11, 2021, https://doi.org/10.3390/s21113894.

[9] B. Radjenovic, M. Sabo, L. Soltes, M. Prnova, P. Cicak, and M. R. Radjenovic, "On Efficacy of Microwave Ablation in the Thermal Treatment of an Early-Stage Hepatocellular Carcinoma," Cancers, vol. 13, no. 22, 2021, https://doi.org/10.3390/cancers13225784.